



Mapping temperature and precipitation climate normals over Bulgaria by using ArcGIS Pro 2.4

Krastina Malcheva, Lilia Bocheva, Tania Marinova

*National Institute of Meteorology and Hydrology,
Tsarigradsko shose 66, 1784 Sofia, Bulgaria*

(Received: 20 Dec 2019, accepted: 7 Feb 2020)

Abstract: Regardless its small territory, Bulgaria has over 20 different climatic regions, so specifying the temperature and precipitation climate normals for the whole territory of the country, including the areas without meteorological monitoring, is an important task. For this purpose, monthly temperature and precipitation normals (1961-1990) for 158 synoptic and climatological stations, and 220 precipitation stations of the meteorological network of the National Institute of Meteorology and Hydrology have been calculated based on thoroughly analyzed archive data. The advanced tools, embedded in ArcGIS Pro 2.4, have been used to elaborate accurate maps of temperature and precipitation climate normals. Some topographic and other climate-related factors that play an essential role in the temperature and precipitation modeling have been explored.

Keywords: climate normals, EBK Regression Prediction, explanatory variables

1. INTRODUCTION

In the light of the current climate change, it is relevant to specify the climate normals about the main meteorological elements, especially about temperature and precipitation, for the whole territory of the country, including the areas without meteorological monitoring. The 30-year period 1961-1990 is the most recent standard reference period as defined by the World Meteorological Organization.

The local and regional temperature and precipitation regimes across the territory of Bulgaria are highly influenced by altitude, topography, the proximity to large water bodies (the Black Sea and the Aegean Sea), and the prevailing atmospheric circulation. The climate of the country represents a transition between two main climate types (Moderate Continental and Mediterranean), in which the intra-annual temperature and precipitation regimes are very different. Northern and Southern Bulgaria are naturally

separated by the Balkan Mountains, which determines their climatic peculiarities. Western Bulgaria is dominated by mountains of various height, shape, size, and orientation. Eastern Bulgaria is relatively flat and borders the Black Sea that has a decisive impact on the local climate. Northern Bulgaria is also rather flat, while the southern areas of the country are more mountainous. The zonal orientation of the Balkan Mountains acts as a natural barrier to the invasion of cold air masses towards the south. This mountain range, along with Rila-Rhodope mountain massif are also a barrier to the penetration of southern warm air masses, which are forced to rise over them. (Sabev&Stanev, 1959).

The present work aims to demonstrate some advanced interpolation techniques in the elaboration of accurate maps of the temperature and precipitation climate normals for the territory of Bulgaria, as well as to explore the topographic and other climate-related factors that play an essential role in the temperature and precipitation modeling.

2. DATA AND METHODS

Monthly precipitation and temperature normals (1961-1990), calculated for 158 synoptic and climatological stations, and 220 precipitation stations of the meteorological network of the National Institute of Meteorology and Hydrology are used in the study (Figure 1).

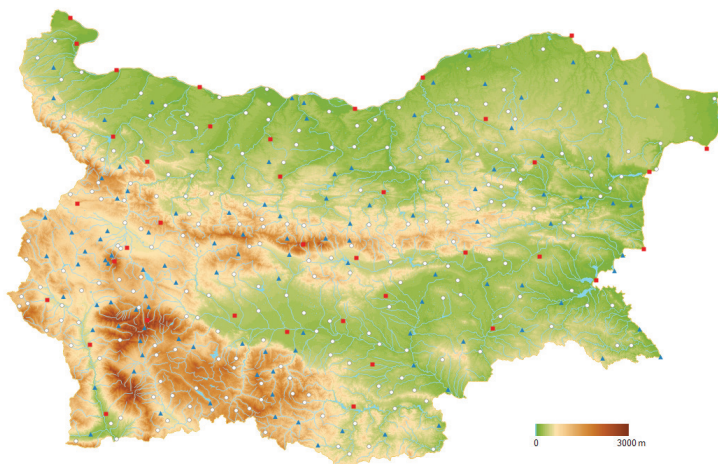


Fig. 1. Hypsometric map of Bulgaria and spatial distribution of the meteorological stations used in the survey: synoptic (red squares), climatological (blue triangles), and precipitation (white circles)

Despite its small territory, Bulgaria has over 20 different climatic regions, so a dense meteorological network, especially for precipitation monitoring, is needed. In the non-mountainous areas, the spatial distribution of weather stations corresponds to the topographic peculiarities, but on a higher altitude, the monitoring network is sparse,

therefore requires the use of advanced interpolation methods to reduce the modeling uncertainty. Also, in the period after 1961, some stations have been moved, but the new data have been added to the previous dataset, supposing that the climatology of the two locations does not differ very much. For this reason, all archive data, including metadata and other information, were thoroughly examined for gaps and errors, and the samples were tested carefully for outliers and spatiotemporal inconsistency. Data quality control was carried out using R software ClimPACT2 (Alexander et al., 2013) and ‘spacetime’ R package (Pebesma, 2012). All calculated monthly normals were compared with those from the reference books, obtained for other periods.

The mapping process comprises the following steps: 1) exploratory regression analysis to select the adequate MLR (Multiple Linear Regression) models, 2) regression kriging interpolation to make the maps and 3) cross-validation. The described steps are performed by using ArcGIS Pro 2.4 tools, so the explanation presented below is based on the ESRI website information (Environmental Systems Research Institute, 2019) as well as on some ESRI researchers’ articles. The detailed mathematical explanation is avoided because a) the spatial statistics tools used for regression analysis are well documented and accessed in a standard fashion and b) the used tools are, practically automated, only require the tuning of a few boundary values but not the user-defined choice of statistical tests or variogram parameters.

2.1. Exploratory regression analysis

MLR is a statistical technique that models the linear relationships between the dependent variable (predictant) and the explanatory variables (predictors) given by the well-known equations:

$$Y_i = \beta_0 + \sum \beta_j X_{ij} + u_i = \mathbf{x}_i^T \boldsymbol{\beta} + \mathbf{u} \quad \text{and} \quad \mathbf{y} = \mathbf{X}\boldsymbol{\beta} + \mathbf{u},$$

where \mathbf{y} is the dependent variable vector; \mathbf{X} is the matrix of the explanatory variables; $\boldsymbol{\beta}$ is the vector of regression coefficients; \mathbf{u} is the vector of residuals.

The Exploratory Regression is a data mining tool that seeks for possible combinations of explanatory variables that satisfy all of the necessary Ordinary Least Squares (OLS) diagnostics under the user-defined criteria about Adjusted R Squared (AdjR2) minimum values, model coefficients p-values, Variance Inflation Factor (VIF) values, Jarque-Bera p-values, and spatial autocorrelation p-values (Rosenshein et al., 2011). The Adjusted R Squared value summarizes the explanatory power of the regression model. The Variance Inflation Factor value, computed for each explanatory variable, is a measure of redundancy and points to the variables that may be removed without losing the model power. The Jarque-Bera statistic indicates whether the model residuals are normally distributed, which is a necessary condition for an adequately specified model. Statistically significant spatial autocorrelation in the model residuals that can be

assessed by Spatial Autocorrelation (Moran's I) tool is linked to the missing of important explanatory variables.

2.2. EBK Regression Prediction

EBK Regression Prediction is a geostatistical interpolation method that combines Empirical Bayesian Kriging (EBK) with regression analysis (Krivoruchko&Gribov, 2019). In the regression models, the explanatory variables often are correlated with each other. The problem of multicollinearity is solved through the transformation of the primary explanatory variables, imperatively in raster format, into their principal components before building the regression model.

EBK Regression Prediction deals with the locally and independently calculated models, dividing the input data into overlapping subsets of a given size that allows the accurate modeling of the spatial changes of the relationships between the explanatory variables and the dependent variable.

The Matérn class of variogram functions is basic for EBK Regression Prediction:

$$\gamma(\mathbf{h}; \boldsymbol{\theta}) = \theta_s \left[1 - \frac{(\Omega_{\theta_k} \|\mathbf{h}\| / \theta_r)^{\theta_k}}{2^{\theta_k-1} \Gamma(\theta_k)} K_{\theta_k} (\Omega_{\theta_k} \|\mathbf{h}\| / \theta_r) \right],$$

where $\theta_s \geq 0$, $\theta_r \geq 0$, $\theta_k \geq 0$, Ω_{θ_k} satisfies the constraint $\gamma(\theta_r) = 0.95\theta_s$ for any θ_k ; $\Gamma(\cdot)$ is the Gama function; $K_{\theta_k}(\cdot)$ is the Bessel function of the second kind and order θ_k ; $\|\mathbf{h}\|$ is the Euclidean length of the lag vector \mathbf{h} . The smoothness varies with $\nu \theta_k$, and the most commonly used parametric variogram models of this class are the Gaussian ($\nu \theta_k = \infty$), Whittle ($\nu \theta_k = 1$) and exponential ($\nu \theta_k = 0.5$). Because of its flexibility, this model gives the most accurate predictions, but it requires the estimation of an additional parameter θ_k and much longer calculation time.

The semivariogram parameters in EBK are estimated using restricted maximum likelihood (Zimmerman, 1991). For each subset, at first, a semivariogram is determined from the local data; new data is simulated at each location in the subset, using this semivariogram as a model, and after that, a new semivariogram is estimated from the simulated data. This process creates a vast number of semivariograms for each subset (Figure 2, left). EBK automates the most challenging aspects of building a valid kriging model by accounting for the error introduced by estimating the underlying semivariogram and avoiding the manual adjustment of parameters (Krivoruchko, 2012).

The cross-validation process in ArcGIS Geostatistical Analyst is based on the consecutive exclusion of data-points that aims to compare the predicted values to the observed values over the whole sample. The cross-validation result (Figure 2, right) comprises the following useful statistics: Mean Error (ME) is the averaged difference between the measured and the predicted values; Root Mean Square Error (RMSE)

indicates how closely the model predicts the measured values; Average Standard Error (ASE) is the average value of the prediction standard errors; Mean Standardized Error (MSE) is the average value of the standardized errors. The average Continuous Ranked Probability Score (CRPS) of all points measures the deviation from the predictive cumulative distribution function to each observed data value. This value should be as small as possible. This diagnostic has advantages over other cross-validation diagnostics because it compares the data to a full distribution rather than to single-point predictions.

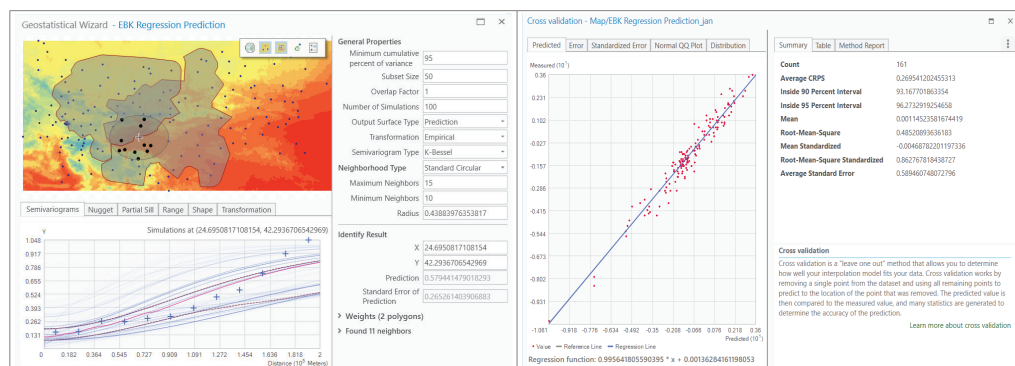


Fig. 2. Screenshots of EBK Regression Prediction steps: model configuration (left) and cross-validation results (right)

2.3. Topography parameters as explanatory variables

Terrain characteristics, as a function of the elevation variability, can be computed from a Digital Elevation Model (DEM). The slope is the rate of change of elevation in the direction of the steepest descent, whereas the first-order partial derivatives – N-S slope and E-W slope – are the slopes in the North-South and East-West directions, respectively. The elevation’s second-order partial derivatives such as profile and tangential curvatures that identify concavity and convexity in the direction of the slope or perpendicular to the slope are often used to characterize locally convex and concave shapes (Hofierka et al., 2009; Neteler&Mitasova, 2013).

The slope and aspect modulate the incoming solar radiation flux, and so affect the microclimate, but the topography-dependent representation of surface temperature in many climate studies determines the elevation as more important than surface shape. The precipitation is best described by a model that permits spatially-varying elevation lapse rates and secondary aspect effects related to prevailing wind directions (Hutchinson&Gallant, 2000). As established in the study of Ranhao et al. (2008), the commonly used topographic variables (altitude, slope, aspect, longitude, and latitude) by themselves or their linear combinations cannot explain the precipitation patterns appropriately, especially in mountainous areas. In Oettli&Camberlin (2005), the

topography was described by quantitative estimates of slopes, the mean and standard deviation of elevation, east-west or north-south exposures, valley/ridge patterns, etc. The authors state that using at most four predictors, between 53 and 89% of the spatial variance of the monthly rainfall fields is explained. The AURELHY (Analyse Utilisant le Relief pour les Bésoins de l'Hydrométéorologie) method has been developed to estimate monthly and annual climatology in France, taking into account the effects of relief through a principal component (PC) analysis of the elevation differences between a large number of neighboring grid points in both latitudinal and longitudinal directions. The first few PCs indicate peaks and valleys, east-west slopes, north-south slopes, and saddles. Additional PCs account for finer relief structures (Bénichou&Breton, 1989; Canellas et al., 2014). In recent years, the potential to use the AURELHY principal components in temperature and precipitation interpolation for the territory of Greece has been investigated, one must read Mamara et al. (2017) and Gofa et al. (2019).

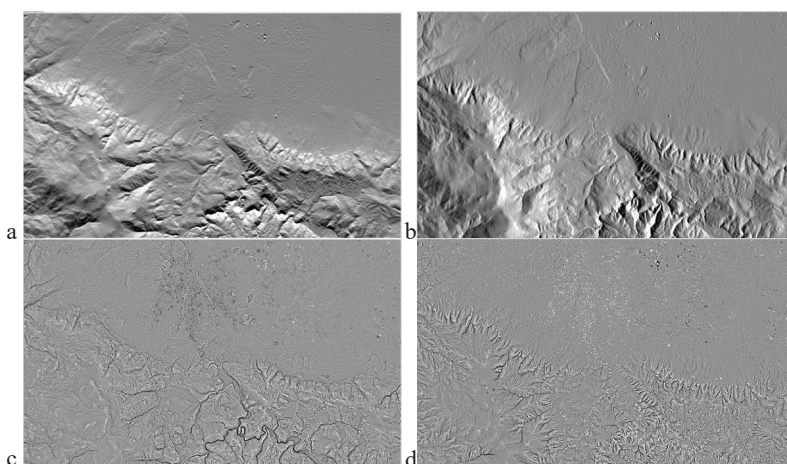


Fig. 3. First-order (a/ and b/) and second-order (c/ and d/) partial derivatives of the digital elevation surface model AW3D30 with an example of Sofia Valley (a flat urban area and a part of the northern slopes of Vitosha Mountain); a/ N-S slopes, b/ E-W slopes; c/ profile curvature; d/ tangential curvature

The embedded *r.slope.aspect* tool in GRASS 7.6 (GRASS homepage, 2019) is used in the current survey to produce the exploratory topographic variables in raster format from the digital model AW3D30 of the Japan Aerospace Exploration Agency (JAXA). This free of charge global digital surface model (DSM) dataset with a horizontal resolution of approximately 30-meter mesh (1 arcsec) has been built on images acquired by the Advanced Land Observing Satellite “DAICHI” (ALOS). The dataset is published based on the DSM data (5-meter mesh version) of the “World 3D Topographic Data”, which is the most precise global-scale elevation data at this time, and its elevation precision is also at a world-leading level as a 30-meter mesh version (JAXA EORC homepage, 2019).

2.4. Climate-related factors as explanatory variables

Continentality is a complex climate characteristic measuring the influence of large water bodies on the regional climate that can improve the geographic sensitiveness of the interpolation. The continentality has been assigned particular importance in the characterization of areas with the so-called transitional climate combining continental and oceanic impacts (Szymanowski et al., 2017). In the study of Hogewind&Bissolli (2011), in which is proposed a method of spatial interpolation of monthly temperature data in WMO Region VI (Europe and Middle East) for preparing operational climate monitoring maps, the expression of continentality index k by Hogewind (2010) is redefined:

$$k = \frac{110 \cdot \text{annual amplitude}}{(\text{latitude } \varphi + 6)},$$

where *latitude* φ is the latitude in decimal degrees; *annual amplitude* ($^{\circ}\text{C}$) is calculated by the difference of the long-term means (1961-1990) of the maximum temperature in summer (from June to August) and that of the minimum temperature in winter (from December to February). This continentality index is classified into four classes: highly maritime (between 0 and 25), maritime (from 26 to 50), continental (from 51 to 75), and highly continental (from 76 to 100). The calculated values for the territory of Bulgaria fall in the range of about 35 to 55 (Figure 4, left).

Aridity is a long-term hydrologic and climatic condition, significant in the context of global climate change, which is mainly the result of large-scale circulation patterns and regional topography (Maliva&Missimer, 2012). In addition to the relevant climate classifications, the aridity indices allow verifying regional climate characteristics in the presence of climate variations. In the present survey, the De Martonne aridity index (De Martonne, 1926), which is based on the annual precipitation and annual mean temperature data, is selected as an explanatory variable in the modeling of precipitation normals:

$$I = \frac{P}{T + 10},$$

where P and T are the long-term averages of the annual precipitation sum and annual mean temperature for the period 1961-1990. Values between 20 and 24 correspond to the Mediterranean climate type. For the territory of Bulgaria, De Martonne aridity index values vary from about 20 to over 130 (Figure 4, right).

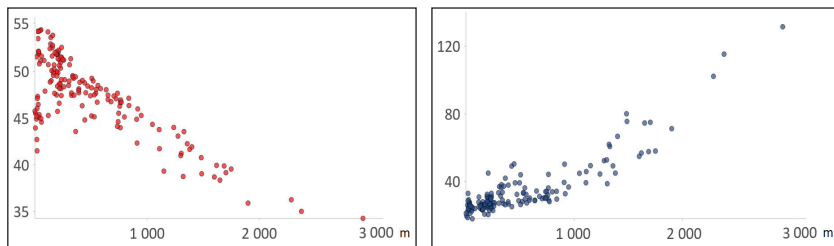


Fig. 4. Scatter plot of the continentality index k (left) and the aridity index I (right) vs. altitude.

High-resolution rasters for the chosen climate-related explanatory variables have been obtained by the EBK Regression Prediction method using the digital model AW3D30 as an elevation data source (Figure 5).

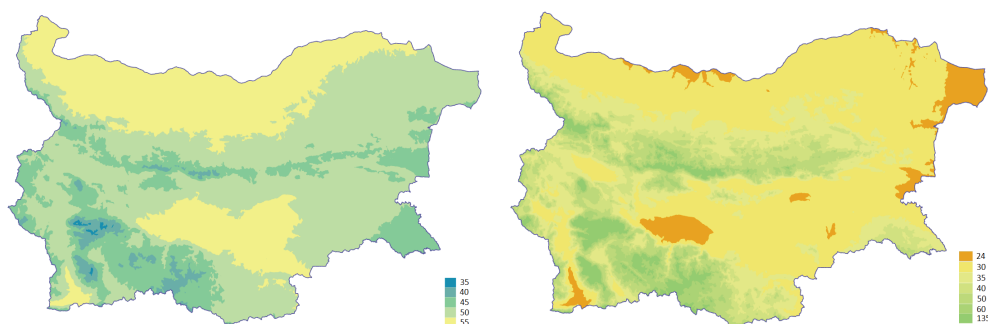


Fig. 5. Spatial distribution of the continentality index k (left) and the aridity index I (right) for the territory of Bulgaria

3. SPATIAL INTERPOLATION OF TEMPERATURE NORMALS (1961-1990)

The results of exploratory regression analysis and EBKR modeling of temperature standard normals are summarized in Figure 6 and Table 1, where ALT_DEM is the altitude derived from the digital surface model; LONG and LAT are longitudinal and latitudinal coordinates; EW_SLOPE, NS_SLOPE, TANGENT, and PROFILE correspond to the described in subsection 2.2.3 topography parameters; CONT_INDEX is the continentality index by Hogewind (2010), as appears in Hogewind & Bissolli (2011). The selected constraints for OLS diagnostics are the following – 50% for AdjR2 values; 7.5 for VIF values; 0.05 for p-values of model coefficients, spatial autocorrelation, and Jarque-Bera test.

The own explanatory power of the chosen predictors for temperature modeling vary of about 0% for secondary topographic parameters to 93.4% for altitude. Latitude and

directional slopes have a weak contribution to some seasons only. The continentality index has a stronger effect in the warm half-year (up to 79.8% in May).

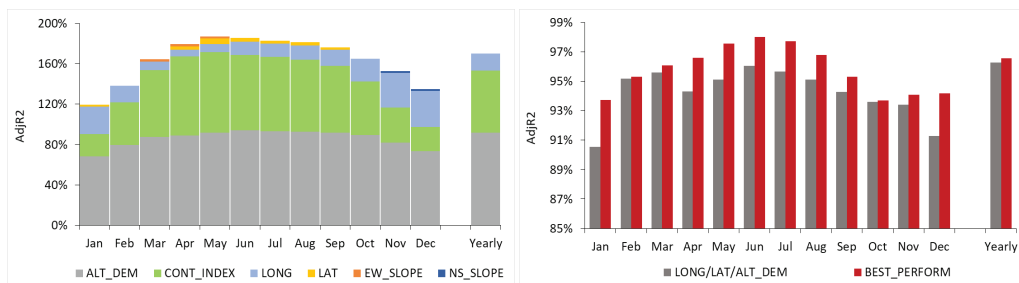


Fig. 6. Left – explanatory power of the chosen predictors for temperature modeling; right – comparison between the regression model with the highest AdjR2 value (BEST_PERFORM) and this one, based only on 3D coordinate data.

The regression models with the highest AdjR2 values (from 93.7% for January to 98% for June) include one or two supplementary predictors besides the longitude, latitude, and altitude, which improves the explanatory power with 0.2-3.2%. RMSEs vary from 0.46 °C in March to 0.63 °C in September. According to the CRPS values after the cross-validation procedure, smaller deviations from the predictive cumulative distribution functions are obtained for the first six months. The tangential curvature modulates the effect of continentality in the interpolation of monthly temperature normals for the second half-year except November, as well as of annual average temperature. The profile curvature takes part in the temperature modeling for April only.

Table 1. Summary information about the structure and cross-validation result of the regression models for temperature with the highest AdjR2

T (°C)	Explanatory Variables					Cross-Validation	
	LAT/LONG	ALT_DEM	CONT_INDEX	TANGENT	PROFILE	RMSE	CRPS
January	✓	✓	✓			0.52	0.285
February	✓	✓	✓			0.47	0.256
March	✓	✓	✓			0.46	0.255
April	✓	✓	✓		✓	0.51	0.283
May	✓	✓	✓			0.48	0.263
June	✓	✓	✓			0.49	0.273
July	✓	✓	✓	✓		0.53	0.297
August	✓	✓	✓	✓		0.59	0.327
September	✓	✓	✓	✓		0.63	0.355
October	✓	✓	✓	✓		0.61	0.344
November	✓	✓	✓			0.55	0.312
December	✓	✓	✓	✓		0.54	0.302
Yearly	✓	✓	✓	✓		0.47	0.263

Inclusion of continentality index as a predictor has a positive effect on the spatial distribution of prediction standard error – between 82 and almost 100% of the values, sampled on a 30-arcsec grid, don't exceed 0.6 °C for the different months. Moreover, the standard error is quite lower in the large mountainous areas in comparison with the regression model built only on topography predictors, as seen in Figure 7 by the example for annual temperature normal.

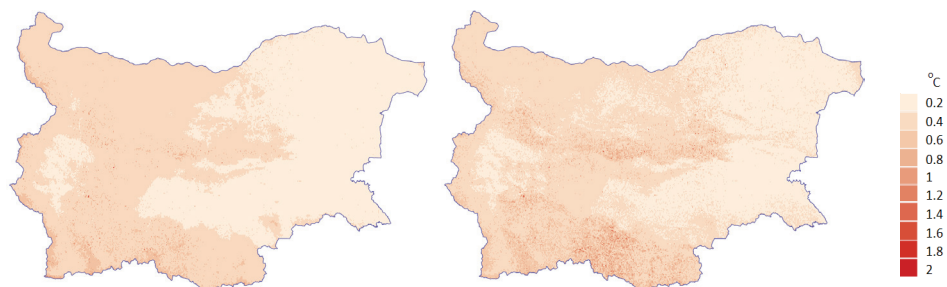


Fig. 7. Prediction standard error maps of annual temperature: regression model that includes the continentality index as a predictor (left); regression model based only on topography predictors (right).

Despite the small latitudinal differences between the northernmost and southernmost regions of the country, the spatiotemporal distribution of the thermal conditions features with considerable diversity and distinct seasonality, determined by the interaction between the intra-annual variability of solar insolation, large scale circulation patterns, and the land surface relief. The altitudinal zoning and the variety of relief forms on the territory of the country contribute to the well-expressed regionalization of temperature features. Figure 8 highlights the spatial patterns of the annual average temperature in the period 1961-1990. The coldest are mountain areas (-3 °C to 8 °C), followed by the high valleys in Western Bulgaria (9 - 10 °C) and the areas, exposed to intense continental invasions in winter, the foothills and hilly regions (10 - 11 °C). The areas with stronger Mediterranean influence are well delineated with temperatures above 12 - 13 °C.

Figure 9 shows the spatial distribution of temperature normals for January and July – the coldest and the warmest month of the year. Outside of mountain regions, where the temperature decreases with altitude (0.3 - 0.4 °C/ 100 m) down to -10.4 °C on the Musala Peak (2925 m), the temperature normal for January is negative in the Danube Plain and high valleys of Western Bulgaria (-3 °C to -0.5 °C). In the Thracian Lowland, Black Sea coastal zone, and Struma Valley, the temperature is positive (up to 3.6 °C along the southern Black Sea coast).

During the summer, the temperatures to the north and the south of the Balkan Mountains are almost equal. July temperature normal ranges in the interval 21 - 24 °C in the Danube Plain and 22 - 24 °C in the Thracian Lowland. The temperature is around or less than 20 °C in the high valleys of Western Bulgaria, about 22 °C on the Black Sea

coast, and 24-25 °C along the Struma Valley. In the mountain areas, the temperature decreases with altitude (0.6-0.7 °C/100 m) down to 4.6 °C on the Musala Peak.

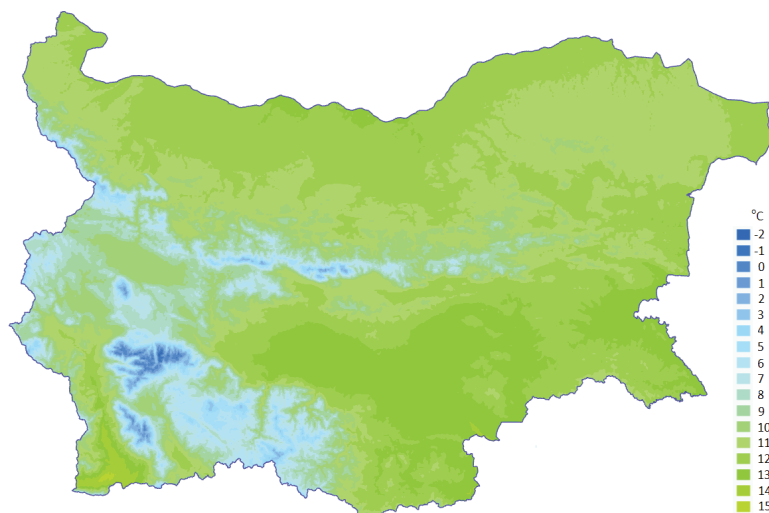


Fig. 8. Spatial distribution of annual temperature climate normal (1961-1990).

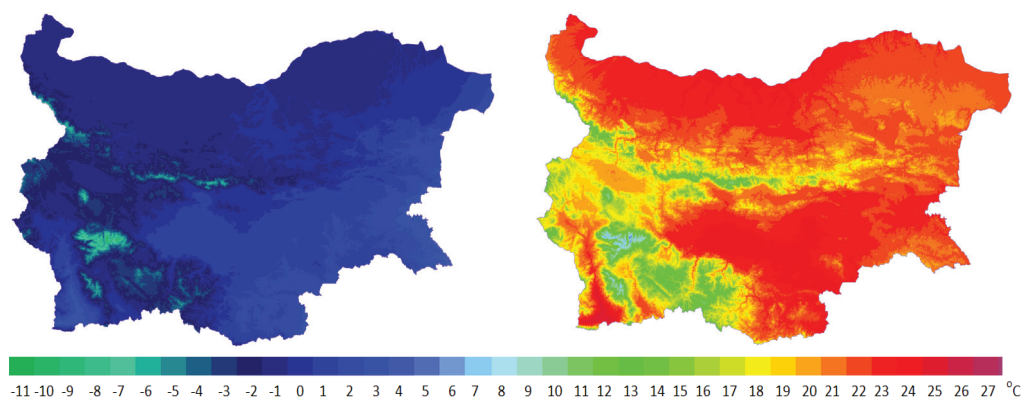


Fig. 9. Spatial distribution of January and July temperature climate normals (1961-1990).

4. SPATIAL INTERPOLATION OF PRECIPITATION NORMALS (1961-1990)

The results of exploratory regression analysis and EBKR modeling of precipitation standard normals are summarized in Figure 10 and Table 2, where ALT_DEM is the altitude derived from the digital surface model; LONG and LAT are longitudinal and

latitudinal coordinates; EW_SLOPE, TANGENT, and PROFILE correspond to the described in subsection 2.3 topography parameters; ARID_INDEX is the De Martonne aridity index. The selected constraints for OLS diagnostics are the same as those used in temperature analysis.

The own explanatory power of the chosen predictors for precipitation modeling vary of about 0% for almost all first and secondary topography parameters except EW_SLOPE to 57.9% for altitude. Latitude and longitude have a distinct seasonal contribution, respectively, in the cold and warm half-year with a maximum of 34% in December for latitude, and 21.4% in May for longitude. The aridity index has a stronger effect in the warm half-year (up to 69.4% in April) but reaches a maximum value for yearly precipitation (73.3%).

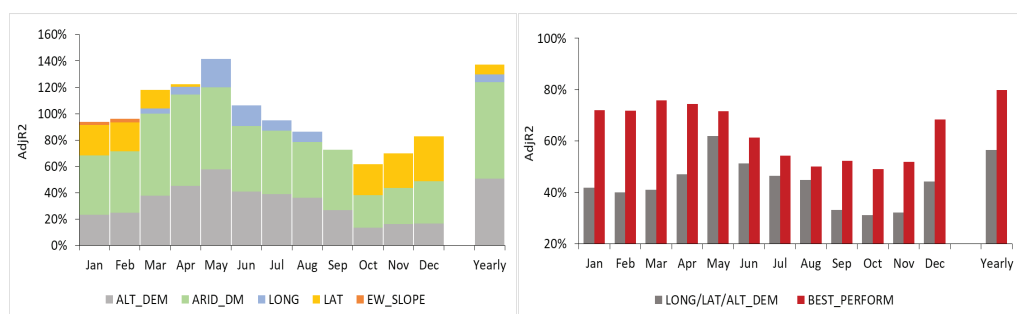


Fig. 10. Left – explanatory power of the chosen predictors for precipitation modeling; right – comparison between the regression model with the highest AdjR2 value (BEST_PERFORM) and this one, based only on 3D coordinate data.

The regression models with the highest AdjR2 values (from 49% for October to 75.9% for March and 79.9% for yearly precipitation) include three or four predictors, which improves the explanatory power with 9.4-34.9% compared to the models built only on data for longitude, latitude, and altitude. RMSEs vary from 5.08 mm in September to 8.36 mm in May.

According to the CRPS values after the cross-validation procedure, the smallest deviations from the predictive cumulative distribution functions are obtained for September and October. The tangential curvature modulates the effect of aridity index in the interpolation of precipitation normals for the months with predominant convective rainfall. The altitude is substituted by the secondary topographic parameters from May to September, but it is implicitly set through the aridity index. The profile curvature takes part in the modeling of yearly precipitation, as well as of monthly precipitation for April and May.

The prediction standard error maps represent the standard errors of the predicted values at each location. Standard error values should be interpreted while keeping in mind the values and range of the input data (Environmental Systems Research Institute, 2019). This is of particular importance for the accuracy assessment of precipitation

modeling results, so a modified standard error (the standard error value divided by the respective predicted value) is used hereafter. De Martonne aridity index, as a predictor, has a positive effect on the spatial distribution of prediction standard error – between 44.5 and 91.6% of the modified standard error values, sampled on a 30-arcsec grid, don't exceed 10% for the different months. Moreover, the error is lower in the mountainous areas, mainly in Western Bulgaria, in comparison with the regression model built only on topography predictors, as seen in Figure 11 by the example for yearly precipitation.

Table 2. Summary information about the structure and cross-validation result of the regression models for precipitation with the highest AdjR2

R (mm)	Explanatory Variables					Cross-Validation	
	LAT/LONG	ALT_DEM	ARID_INDEX	TANGENT	PROFILE	RMSE	CRPS
January	✓	✓	✓			7.24	3.523
February	✓	✓	✓			7.35	3.422
March	✓	✓	✓			6.37	3.257
April	✓	✓	✓		✓	6.03	3.098
May	✓		✓		✓	8.36	3.988
June	✓		✓	✓		8.09	3.974
July	✓		✓	✓		6.91	3.439
August	✓		✓	✓		6.49	3.246
September	✓		✓	✓		5.08	2.534
October	✓	✓	✓			5.79	2.742
November	✓	✓	✓			7.89	3.785
December	✓	✓	✓			8.25	3.870
Yearly	✓	✓	✓		✓	62.22	30.797

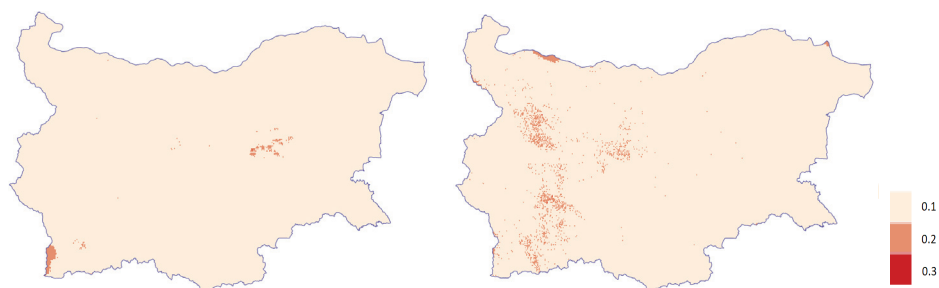


Fig. 11. Modified prediction standard error maps (the standard error values divided by the respective predicted values) of annual precipitation: regression model that includes the aridity index as a predictor (left); regression model based only on topography predictors (right).

The annual course of precipitation is closely related to the peculiarities of atmospheric circulation over the country and sharply differs in the areas under the continental and Mediterranean influence. Average annual values of precipitation in the period 1961-

1990 vary from 400-500 mm in the Black Sea coastal zone, some parts of the Danube Plain, and Thracian Lowland to over 1100 mm in the mountainous areas (Figure 12). The annual precipitation increases linearly with altitude up to 2000 m in the mountains (country averaged 20-40 mm/100 m).

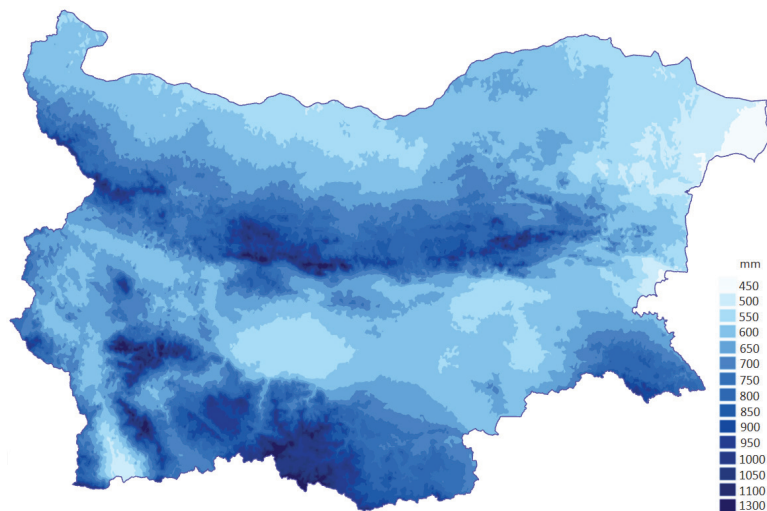


Fig. 12. Spatial distribution of annual precipitation climate normal (1961-1990).

The 1961-1990 precipitation normals for December, the wettest month of the year in the regions with strong Mediterranean influence, as well for June – the wettest month in the areas with a continental climate, are shown in Figure 13.

In the regions with continental climate (the Danube Plain, the slopes of the Balkan Mountains, Vitosha, the high valleys of Western Bulgaria, and the northern slopes of the Rila-Rhodope Massif), the December precipitation normal varies from about 30 to 60 mm in the lowlands and to 80-120 mm in the mountainous areas. In the southern areas with strong Mediterranean influence (the eastern parts of Rhodopes and Strandzha, along the river valleys and south Black Sea coastal zone), the precipitation in December alters from 60-70 mm to over 130 mm.

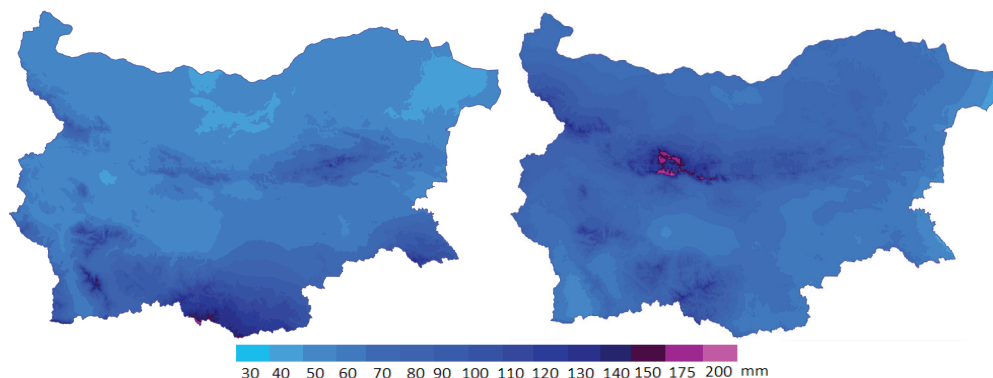


Fig. 13. Spatial distribution of December and June precipitation climate normals (1961-1990).

In the areas with a continental climate, the precipitation maximum is in June (from 40-60 mm to over 150 mm). In the southern regions, the summer precipitation is the smallest (about 20% of the annual amount). In June, the precipitation varies from 30-50 mm to over 120 mm in the mountains.

5. CONCLUDING REMARKS

Despite its small territory, Bulgaria has more than 20 different climatic regions, and therefore, in the light of the current climate change, it would be very useful to specify the climate normals concerning the main meteorological elements, such as temperature and precipitation. In this context, the primary objective of the paper was to perform spatial interpolation, using advanced tools embedded in ArcGIS 2.4 (and especially, the Empirical Bayesian Kriging Regression Prediction), for obtaining accurate maps of temperature and precipitation climate normals.

The generated maps adequately describe the spatial and intra-annual variability of temperature and precipitation fields. The regression models with the highest performance for temperature modeling (from 93.7% for January to 98% for June) include one or two supplementary predictors besides the longitude, latitude, and altitude, which improves the explanatory power with 0.2-3.2%. RMSEs vary from 0.46 °C in March to 0.63 °C in September. Inclusion of continentality index as a predictor has a positive effect on the spatial distribution of prediction standard error, especially in the large mountainous areas – between 82 and almost 100% of the values, sampled on a 30-arcsec grid, don't exceed 0.6 °C for the different months.

The regression models with the highest performance for precipitation modeling (from 49% for October to 75.9% for March and 79.9% for yearly precipitation) include three or four predictors, which improves the explanatory power with 9.4-34.9% compared to the models built only on data for longitude, latitude, and altitude. RMSEs vary from

5.08 mm in September to 8.36 mm in May. De Martonne aridity index, as a predictor, has a positive effect on the spatial distribution of prediction standard error – between 44.5 and 91.6% of the error values, sampled on a 30-arcsec grid, don't exceed 10% for the different months. In future studies, the number of predictors will be expanded to allow more accurate modeling of precipitation fields.

REFERENCES

- Bénichou, P. and Le Breton, O. (1989). AURELHY: une méthode d'analyse utilisant le relief pour les besoins de l'hydrométéorologie. In Deuxièmes journées hydrologiques de l'ORSTOM à Montpellier; ORSTOM: Marseille, France, 1989; pp. 299-304
- Broccoli, A. J. and Manabe, S. (1992). The effects of orography on midlatitude Northern Hemisphere dry climates. *J. Climate*, 5, 1181-1201
- Canellas C., Gibelin A.L., Lassègues P., Kerdoncuff M., Dandin P., and Simon P. (2014). Les normales climatiques spatialisées Aurelhy 1981–2010: Températures et précipitations. *La Météorol.* 2014, 85, pp. 47-55
- De Martonne, E. (1926). Une nouvelle fonction climatologique: L'indice d'aridité. *La Meteorologie*, 449-458
- Environmental Systems Research Institute (2019). ArcGIS Pro Help. Redlands, CA, <https://pro.arcgis.com/en/pro-app/help/main/welcome-to-the-arcgis-pro-app-help.htm>
- Gofa F., Mamara A., Anadranistakis M., and Flocas H. (2019). Developing Gridded Climate Data Sets of Precipitation for Greece Based on Homogenized Time Series. *Climate*, 7, 68
- GRASS homepage (2019), <http://grass.osgeo.org>
- Hofierka J., H. Mitasova, and Neteler M. (2009). Geomorphometry in GRASS GIS. In: Hengl, T. and Reuter, H.I. (Eds), *Geomorphometry: Concepts, Software, Applications. Developments in Soil Science*, vol. 33, pp. 387-410. Elsevier, ISBN: 978-0-123-74345-9
- Hogewind, F. and P. Bissolli (2011). Operational maps of monthly mean temperature for WMO Region VI (Europe and Middle East). *IDŐJÁRÁS*, Vol. 115, 1-2, pp. 31-49
- Hogewind, F. (2010). *Raum-zeitliche Analyse der Klimavariabilität anhand von hochaufgelösten interpolierten Klimakarten am Beispiel von Europa und dem Nahen Osten (Region VI der Weltorganisation für Meteorologie)*. PhD thesis, University of Mainz, Germany).
- Hutchinson, M.F. and Gallant, J.C. (2000). Representation of terrain, in J.P. Wilson and J.C. Gallant (Eds.). *Terrain Analysis: Principles and Applications*. Wiley, ISBN: 978-0-471-32188-0
- JAXA EORC (2016). ALOS Global Digital Surface Model “ALOS World 3D - 30m” (AW3D30), <http://www.eorc.jaxa.jp/ALOS/en/aw3d30/index.htm>
- Krivoruchko, K. (2012). Empirical, Bayesian Kriging: Implemented in ArcGIS Geostatistical Analyst ArcUser Magazine, Fall 2012, pp. 6-10, Redlands, CA: Environmental Systems Research Institute, <http://www.esri.com/news/arcuser/index.html>
- Krivoruchko, K., Gribov, A., 2019. Evaluation of empirical Bayesian kriging. *SpatialStatistics* 32, 100368. <https://doi.org/10.1016/j.spasta.2019.100368>
- L. Alexander, H. Yang, and S. Perkins, *ClimPACT—Indices and Software*, 2013, http://www.wmo.int/pages/prog/wcp/ccl/opace/opace4/meetings/documents/ETCRSCI_software_documentation_v2a.doc

- Maliva, R. and Missimer, T. (2012). *Arid Lands Water Evaluation Management*. Berlin, Springer, ISBN: 978-3-642-29104-3
- Mamara, A., Anadranistakis, M., Argiriou, A. A., Szentimrey, T., Kovacs, T., Bezes, A., and Bihari, Z. (2017). High resolution air temperature climatology for Greece for the period 1971–2000. *Meteorological Applications*, 24 (2), 191-205
- Neteler, M. and H. Mitasova (2013). *Open source GIS: a GRASS GIS approach*. Springer Science & Business Media. SECS, volume 689
- Oettli, P. and P. Camberlin (2005). Influence of topography on monthly rainfall distribution over East Africa, *Clim. Res.*, 28 (3), 199-212
- Pal, J. S. and E. A. B. Eltahir (2003). A feedback mechanism between soil moisture distribution and storm tracks. *Quart. J. Roy. Meteor. Soc.*, 129, 2279-2297
- Pebesma, E. (2012), *Spacetime: Spatio-temporal data in R*, *J. Stat. Software*, 51, 1–30.
- Ranhao S., Z. Baiping and T. Jing (2008). A multivariate regression model for predicting precipitation in the Daqing Mountains. *Mt Res Dev* 28, pp. 318-325
- Rosenshein L., L. Scott, and M. Pratt (2011). *Finding a Meaningful Model*, *ArcUser Magazine*, Winter 2011, pp. 40-45, Redlands, CA: Environmental Systems Research Institute, <http://www.esri.com/news/arcuser/index.html>
- Sabev, L. and Stanev S. (1959). *Climatic Dividing into Districts of Bulgaria*, Scientific works of the Institute of Hydrology and Meteorology, vol. 5, Nauka i izkustvo, Sofia (in Bulgarian)
- Sturman, A. and Wanner H. (2001). *A Comparative Review of the Weather and Climate of the Southern Alps of New Zealand and the European Alps*. *Mountain Research and Development*, 21(4), 359-369
- Szymanowski, M., Bednarczyk, P., Kryza, M. et al. *Spatial Interpolation of Ewert's Index of Continentality in Poland*. *Pure Appl. Geophys.* (2017) 174, 2: 623–642.
- Zimmerman, Dale L. & M. Bridget Zimmerman (1991) *A Comparison of Spatial Semivariogram Estimators and Corresponding Ordinary Kriging Predictors*, *Technometrics*, 33:1, 77-91, DOI: 10.1080/00401706.1991.10484771